

Thirty years of tephra erosion following the 1980 eruption of Mount St. Helens

Brian D. Collins^{1*}  and Thomas Dunne² 

¹ Department of Earth and Space Sciences, University of Washington, Seattle, WA 98195, USA

² Bren School of Environmental Science and Management & Department of Earth Science, University of California, Santa Barbara, Santa Barbara, CA 93106, USA

Received 6 October 2018; Revised 15 July 2019; Accepted 22 July 2019

*Correspondence to: B. D. Collins, Department of Earth and Space Sciences, University of Washington, Seattle, WA 98195, USA. E-mail: bcollins@uw.edu

ESPL

Earth Surface Processes and Landforms

ABSTRACT: Repeated measurement of tephra erosion near Mount St. Helens over a 30-year period at steel stakes, installed on 10 hillslopes in the months following the 1980 eruption, provides a unique long-term record of changing processes, controls and rates of erosion. Intensive monitoring in the first three post-eruption years showed erosion declined rapidly as processes shifted from sheetwash and rilling to rainsplash. To test predictions about changes to long-term rates and processes made based on the 3-year record, we remeasured sites in 1992, 2000 and 2010. Average annual erosion from 1983 to 1992 averaged 3.1 mm year^{-1} and ranged from 1.4 to 5.9 mm year^{-1} , with the highest rate on moderately steep slopes. Stakes in rills in 1983 generally recorded deposition as the rills became rounded, filled and indistinct by 1992, indicating a continued shift in process dominance to rainsplash, frost action and bioturbation. Recovering plants, where present, also slowed erosion. However, in the second and third decades even unvegetated hillslopes ceased recording net measurable erosion; physical processes had stabilized surfaces from sheetwash and rill erosion in the first few years, and they appear to have later stabilized surfaces against rainsplash erosion in the following few decades. Comparison of erosion rates with suspended sediment flux indicates that within about 6 years post-eruption, suspended sediment yield from tephra-covered slopes was indistinguishable from that in forested basins. Thirty years after its deposition, on moderate and gentle hillslopes, most tephra remained; in well-vegetated areas, plant litter accumulated and soil developed, and where the surface remained barren, bioturbation and rainsplash redistributed and mixed tephra. These findings extend our understanding from shorter-term studies of the evolution of erosion processes on freshly created substrate, confirm earlier predictions about temporal changes to tephra erosion following eruptions, and provide insight into the conditions under which tephra layers are preserved. © 2019 John Wiley & Sons, Ltd.

KEYWORDS: tephra erosion; rainsplash erosion; hillslope erosion; erosion in volcanic areas; Mount St. Helens; landscape disturbance

Introduction

Studying the processes, controls and timing of accelerated water and sediment releases from tephra-covered hillslopes clarifies the evolution of erosional processes and the characteristic timescales of erosion episodes and watershed recovery following landscape disturbances of various types (e.g. Moody and Martin, 2001; Moody and Kinner, 2006; Rathburn *et al.*, 2018). It is also important for predicting and mitigating volcanic sedimentation hazards around active volcanoes, which can elevate sediment loads, contributing to downstream sedimentation and flood hazards (for a review, see Pierson and Major, 2014), and for understanding the survival of tephra in the stratigraphic record.

Insights from studies conducted over a few years and several decades are necessary for each purpose. While there are few long-term field studies of tephra erosion, the scientific understanding of post-eruption erosion in the short term is relatively robust, and is based on studies following eruptions at several volcanoes, including: Vulcan, New Guinea (1937); Paricutin, Mexico (1943–1952); Sakurajima, Japan (1955–present); Irazu,

Costa Rica (1963–1965); Usu, Japan (1977–1978, 2000); Mount St. Helens, USA (1980); Pinatubo, Philippines (1991); Unzen, Japan (1991–1995); Miyakejima, Japan (2000); Kasatochi, USA (2008); Chaiten, Chile (2008); Colima, Mexico (1998); and Shinmoe-dake, Japan (2011).

Surfaces of newly created tephra deposits typically have infiltration rates that vary roughly with tephra grain size (Figure 4 of Pierson and Major, 2014) and are low relative to rainfall intensities and to pre-eruption infiltration rates because tephra surface layers often have a fine grain size and laminated, aggregate-poor structure (Collins and Dunne, 1986; Leavesley *et al.*, 1989; Ikeya *et al.*, 1995; Miyabuchi *et al.*, 1999; Yamakoshi and Suwa, 2000; Yamakoshi *et al.*, 2005; Ogawa *et al.*, 2007; Teramoto and Shimokawa, 2010). Infiltration rates are low, even where fine-textured layers are only a few millimetres thick (Teramoto *et al.*, 2006; Ogawa *et al.*, 2007) or where a surface crust develops on coarser deposits (Seegerstrom, 1956; Waldron, 1967; Kadomura *et al.*, 1983; Swanson *et al.*, 1983; Smith and Swanson, 1987). The resulting overland flow causes intense sheetwash and rill erosion, especially on the steep terrain around most volcanoes, and networks of rills and gullies form

in the first precipitation events following tephra eruption (e.g. Waldron, 1967; Yamamoto, 1984; Collins and Dunne, 1986; Waythomas *et al.*, 2010). Rates of sheet and rill erosion vary spatially with slope steepness, deposit grain size and the cover provided by eruption-killed vegetation (e.g. Segerstrom, 1956; Waldron, 1967; Collins *et al.*, 1983; Collins and Dunne, 1986; Smith and Swanson, 1987).

Whereas in prolonged eruptive periods infiltration rates can remain low and erosion can remain rapid (e.g. Shimokawa *et al.*, 1989), after single eruptions erosion rates decline rapidly, as early as during the first post-eruption year (Collins *et al.*, 1983; Yamamoto, 1984; Chinen and Kadomura, 1986; Collins and Dunne, 1986; Smith and Swanson, 1987; Inbar *et al.*, 2001; Shimokawa *et al.*, 1996). Rill erosion slows as the rill network stabilizes and evolves to fewer, master rills (Segerstrom, 1960; Ollier and Brown, 1971; Collins and Dunne, 1986), as rills incise to more permeable and less erodible layers (Chinen and Kadomura, 1986; Collins and Dunne, 1986; Leavesley *et al.*, 1989; Chinen and Riviere, 1990), and later as inter-rill infiltration increases and runoff declines. Sheetwash erosion slows as changes to the inter-rill surface, including erosional armouring and stripping of fine-grained surface layers and coarsening by freeze–thaw and bioturbation, increase infiltration (Leavesley *et al.*, 1989; Yamakoshi and Suwa, 2000; Major and Yamakoshi, 2005; Teramoto *et al.*, 2006; Ogawa *et al.*, 2007) and decrease erodibility (Kadomura *et al.*, 1978; Collins and Dunne, 1986; Teramoto *et al.*, 2006). As overland flow diminishes, the role of rainsplash erosion becomes relatively more important, and rills begin to fill (Yamamoto, 1984; Collins and Dunne, 1986) and rill and gully divides become rounded (Segerstrom, 1966; Collins and Dunne, 1986).

While pathways of plant succession on tephra are complex, highly variable and dependent on spatial heterogeneities in biotic and abiotic conditions (for a review, see del Moral and Grishin, 1999; Crisafulli and Dale, 2018), common findings on the interactions between erosion and initial revegetation have emerged from observations at volcanoes in a variety of environments. The rapid slowing of tephra erosion in the first few post-eruption years preceded vegetative recovery following several eruptions including Paricutin (Eggler, 1959; Segerstrom, 1960), Vulcan (Ollier and Brown, 1971), Usu (Chinen, 1986) and Mount St. Helens (Collins and Dunne, 1986). Revegetation in the first post-eruption years is commonly dominated by secondary succession of buried plants (Griggs, 1919a; Eggler, 1959; Hendrix, 1981; Tsuyuzaki, 1987; Halpern *et al.*, 1990), which remained viable for at least 3 years after tephra burial at Katmai (Griggs, 1919a) and for at least 8 years at St. Helens (Zobel and Antos, 1992). Tephra erosion promotes secondary succession of these buried plants by exposing, or thinning the tephra depth above, the buried soil (Griggs, 1918, 1919a; Eggler, 1959, 1963; Collins and Dunne, 1986, 1988; Chinen and Riviere, 1990); succession is more rapid on steeper slopes where erosion is greater (Lawrence and Ripple, 2000) and on the margins of eruption-affected areas where the tephra layer is thin (e.g. Griggs, 1919a; Hendrix, 1981; Halpern *et al.*, 1990; Inbar *et al.*, 1994; Grishin *et al.*, 1996; Lawrence and Ripple, 2000). Primary succession on the tephra surface is limited in the first few years (Griggs, 1919b; Eggler, 1959, 1963; Gil-Solórzano *et al.*, 2009) but is promoted by the erosional exposure of buried soil (Griggs, 1919b; Collins and Dunne, 1988; Tsuyuzaki, 1994).

Large proportions of erupted tephra can remain stored on hillsides after erosion slows in the first post-eruption years. For example, 3 years after the 1980 eruption of Mount St. Helens, 85% of tephra remained on hillslopes in the Toutle River drainage (Collins and Dunne, 1986), 88% remained a year after the eruption in a 2.4 km² basin in the Clearwater

Creek drainage (Smith and Swanson, 1987) (Figure 1) and 87% of tephra remained 4 years after the 1977–1978 eruption of Usu Volcano (Chinen and Kadomura, 1986). Larger percentages of tephra deposits were eroded from two volcanoes subject to more intense rainfall: Waldron (1967) estimated that 50–67% of tephra remained in 1964 after the second rainy season following the 1963–1965 eruption of Irazu in tropical humid Costa Rica and Segerstrom (1956, Table 10) estimated that sheetwash erosion, in the humid subtropical climate of Paricutin, Mexico, by 1946 had removed 48% of the tephra erupted in 1943. However, in a variety of climates, surface erosion and landslides within the first few post-eruption years stripped entire tephra layers, as thick as 1–6 m at Paricutin (Segerstrom, 1956) from hillslopes with gradients exceeding ~0.70 (e.g. Griggs, 1919b; Segerstrom, 1956, 1960; Kadomura *et al.*, 1983; Smith and Swanson, 1987).

Hillslope tephra erosion is believed to be a short-term source of post-eruption sediment relative to channel network development and channel widening in valley-filling deposits (Lehre *et al.*, 1983; Gran *et al.*, 2011; Pierson and Major, 2014), but this generalization is extrapolated from short-term tephra erosion studies and inference from suspended sediment studies (Major *et al.*, 2000; Gran *et al.*, 2011). Excepting Paricutin, which was observed periodically over nearly 20 years by Segerstrom (1956, 1960, 1966) and El Chichon (observed over 17 years; Inbar *et al.*, 2001), tephra erosion studies spanning more than several years have generally been retrospective interpretations. Field observations made by Inbar *et al.* (1994) decades after Paricutin's eruptive period indicate that sedimentation remained above pre-eruption rates, although the sediment source was not identified. Observations by Ollier and Brown (1971), made decades after a scoria cone formed in 1937 in New Guinea, inferred that gullies had formed initially as shallow rills initiated by surface runoff, enlarged and extended by subsurface seepage, but thereafter remained unchanged beyond the first 'few years' after the eruption. A decade after the 1978 eruption of Tarumae Volcano, Hokkaido, erosion was dominated by freeze–thaw in autumn and early winter in the subpolar environment, resulting in one to two orders of magnitude more sediment than rainsplash during heavy summer rainfall (Miyabuchi and Nakamura, 1991). In general, however, it remains difficult to recognize and generalize about whether, for any particular active volcano, the volume of tephra deposited by eruptions through time on surrounding landforms is increasing or decreasing.

To address the scarcity of long-term tephra erosion studies, we report and interpret erosion measurements made over a 30-year period following the 1980 eruption of Mount St. Helens. After intensive measurements in the 1980–1983 period, we made a projection of future rates based on the argument that physical alteration of the disturbed landscape, rather than revegetation, had stabilized the surface against sheetwash erosion, generally in accord with Horton's (1945) theory of stable drainage densities (Collins and Dunne, 1986). The argument for stabilization was based on both reductions in erosion rates and the fact that rills were being smoothed out of existence, as would be expected with a shift from sheetwash to rainsplash, and as illustrated experimentally by Dunne and Aubry (1986). However, precipitation intensities had not been exceptional, and it left open the possibility that increases in rainfall would rejuvenate the rill network or that some other disturbance, such as trampling by elk herds, would cause either significant temporal fluctuations or even a reversal of the trend in erosion rate. We remeasured the erosion to determine whether any such trends or reversals had occurred, or to strengthen the conclusion that water-driven hillslope erosion of tephra deposits is indeed a short-lived source of sediment to streams.

Study area

The 1980 eruption resulted in several types of deposits (Figure 1). Failure of the volcano's north slope deposited a 2.5 km³ debris avalanche into the North Fork Toutle River drainage (Voight *et al.*, 1981; Glicken, 1996); within 7 km of the volcano, this valley-filling deposit was overlain later in the 1980 eruption by pyroclastic flows (Hoblitt *et al.*, 1981). Lahars were generated by pyroclastic flows on the volcano flanks (Janda *et al.*, 1981; Pierson, 1985; Fairchild, 1987; Scott, 1988; Waite, 1989) and by liquefaction of the North Fork Toutle debris avalanche (Janda *et al.*, 1981; Fairchild, 1987), leaving deposits on the southern slopes of the volcano and along the South Fork and North Fork Toutle valleys. A laterally directed pyroclastic surge knocked down trees in a 550 km² area, 350 km² of this within the Toutle River basin (Figure 1), and deposited gravel to silt-sized sediment (also referred to as 'lateral blast' deposits) on hillslopes (Hoblitt *et al.*, 1981; Waite, 1981; Ongaro *et al.*, 2011), ranging in thickness from 1 m at 10 km to 0.02 m at 25 km from the volcano (Collins and Dunne, 1986). The ash plume from a Plinian eruption subsequent to the lateral surge deposited several centimetres of silt-sized tephra (Waite, 1981; Waite and Dzurisin, 1981). Erosion of these pyroclastic surge and airfall deposits from hillslopes north of the volcano in the Toutle River drainage is the subject of this study.

Forests are in the Douglas fir (*Pseudotsuga menziesii*) and Pacific silver fir (*Abies amabilis*) zones at lower and higher elevations, respectively (Franklin and Dyrness, 1973). Intensive logging in the 40 years preceding the 1980 eruption created a patchwork of old-growth forest, young managed stands and recent clearcuts. The lateral blast killed the above-ground portions of nearly all plants. Trees were uprooted and removed from many slopes facing, and within about 13 km of, the

volcano; on hillslopes sheltered from the blast and at distances up to 28 km from the volcano, trees were uprooted or snapped, but remained on the slope. Near to the volcano, the lateral surge scoured the upper soil horizons, or the entire soil profile, but in most of the affected area, and at all of our study sites, soil was not scoured by the lateral surge deposits. Beyond the limit of downed forest, trees remained standing but were killed in a 0–4 km band (Figure 1). The US Soil Conservation Service applied a mix of grass and legume seeds with fertilizer to 82.5 km² of the blast-affected zone in September and October 1980 (Collins and Dunne, 1988). Destroyed forests were salvage logged during 1980–1982 on private and state land, while the landscape was preserved, including the eruption-destroyed forests, on much of the land within the federal National Volcanic Monument created in 1982 (Figure 1).

Annual precipitation in water year (WY) 1987–2011 averaged 2274 mm year⁻¹ at the Spirit Lake SNOTEL station (USDA NRCS), the nearest weather station to our study sites, 5 km WSW of the Coldwater sites, at elevation 1073 m (Figure 1); on average, 75% of this precipitation fell between 1 October and 31 March (Table I). Rainstorms are generally long and of low intensity; at the nearest precipitation gauge with a reliable record throughout the 30-year study period, Cougar 4 SW (NOAA, 2015) (Figure 1), the 2-year, 1-h and 10-year, 1-h intensities for WY 1980–2011 were 16 and 28 mm h⁻¹, respectively, somewhat greater than predictions for our study area by Miller *et al.* (1973), and the maximum intensity was 33 mm h⁻¹ (Table I). Infiltration capacities measured on the tephra increased from 2 to 5 mm h⁻¹ in 1980 and 4–7 mm h⁻¹ in 1981 (Leavesley *et al.*, 1989) to 9–25 mm h⁻¹ in 2000 (Major and Yamakoshi, 2005); comparison of these infiltration rates to measured precipitation intensities implies that runoff would initially have been frequent but two decades later would have been limited to rare, intense storms.

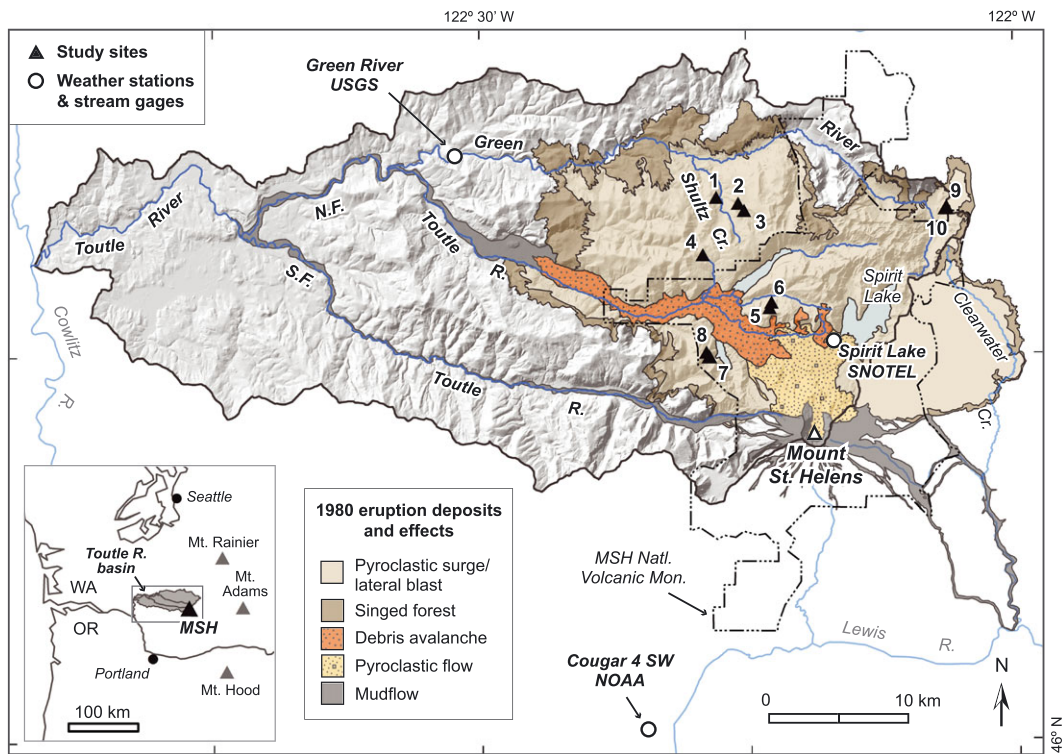


Figure 1. Inset map shows location of Mount St. Helens (MSH), the Toutle River basin and nearby volcanoes in the Cascade Range in southwest Washington and northeast Oregon. Main map shows deposits and effects of the 1980 eruption and study sites in the lateral blast-affected portion of the Toutle River basin: 1, Shultz 1; 2, Shultz 2; 3, Shultz 3; 4, Maratta; 5, Coldwater 1; 6, Coldwater 2; 7, Castle 1; 8, Castle 2; 9, Green 1; 10, Green 2. Map units are generalized from Plate 1 of Lipman and Mullineaux (1981). Also shown: boundary of the Mount St. Helens National Volcanic Monument and locations of weather (Spirit Lake SNOTEL, Cougar 4 SW) and stream gauge (USGS) stations. [Colour figure can be viewed at wileyonlinelibrary.com]

Table I. Characteristics of temperature, precipitation and snow cover at the Spirit Lake SNOTEL (elevation 1073 m) and Cougar 4 SW (elevation 158 m) weather stations (Figure 1) and from Miller *et al.* (1973)

Climate attribute	WY 1987–2011 Spirit Lake SNOTEL	WY 1980–2011 Cougar 4 SW	Miller <i>et al.</i> (1973)
Annual precipitation, average and range (mm year ⁻¹)	2274 (1326–3533)	—	—
Percentage of annual precipitation in 1 October–31 March, average and range (%)	75 (58–85)	—	—
Maximum 1-h precipitation (mm h ⁻¹)	—	33	—
2-year, 1-h precipitation (mm h ⁻¹)	—	16	14
10-year, 1-h precipitation (mm h ⁻¹)	—	28	20
50-year, 1-h precipitation (mm h ⁻¹)	—	—	27
Average daily temperature (°C)	6	—	—
Average daily minimum temperature (°C)	3	—	—
Average daily maximum temperature (°C)	11	—	—
Days per year daily temperature ranges above and below 0 °C, average and range	97 (38–137)	—	—
Days per year of snow cover, average and range (WY 2008–2011 only)	127 (68–157)	—	—

Daily temperature at the Spirit Lake station in WY 1987–2011 averaged 6°C and minimum daily and maximum daily temperatures averaged 3 and 11°C, respectively (Table I). Diurnal air temperature ranged above and below 0°C for 97 days year⁻¹, or 28% of days having observations, indicating that freeze–thaw of the ground surface could have been frequent, although on relatively few of these days (13 days year⁻¹, on average) was the ground not snow covered; snow cover at the Spirit Lake station averaged 127 days year⁻¹ in WY 2008–2011. Our field observations in the first three post-eruption years indicate that at lower elevations snow cover was more intermittent and freeze–thaw cycles may thus have been more frequent.

Methods

In 1992, 2000 and 2010, we measured erosion at steel stakes, 75 cm long and 1.3 cm in diameter, that had been driven into the underlying soil in September and October 1980 (excepting one site, Shultz 3, installed in August 1981) and measured repeatedly during 1980–1983. Stakes were installed in transects along contours; in each transect, 40 stakes were spaced at 2 or 5 m intervals. These transects were spaced at intervals of 10, 20, 40, 60 and 80% of the distance from ridge crest to valley bottom on slopes 180 to 725 m long (Table II). In addition, at seven of these sites, two transects were installed along the fall line, from ridge crest to base of the slope; in each of these transects, 50 stakes were spaced at even intervals. We interpret

net erosion from each site to equal export of sediment from the hillside; while tephra mobilized by erosion could locally redeposit, such sites of local redeposition were sampled by the stake arrays.

Stake arrays sampled hillslopes with average gradients between 0.16 and 0.66 (Table II); all hillslopes had a laterally planar, uncomplicated shape, and in longitudinal form were generally planar or mildly concave or convex (Collins, 1984). Surge deposits on our sites (see Collins and Dunne, 1986 for details) were 0.2–0.5 m thick and texturally fined upward; on the Coldwater sites (Figures 1 and 2), nearest to the volcano, the basal layer was a massive gravelly sand to sandy gravel, with wood and reworked pre-eruption soil incorporated locally at the base. On sites farther from the volcano, the basal layer was a massive, coarse to medium sand overlain by stratified, medium to fine sand. On all sites, this basal layer was overlain by a stratified medium to fine sand. The overlying airfall layer was a sandy silt with accretionary lapilli and while locally as thick as 0.10 m, averaged 0.03–0.06 m. On seven sites, the forest had been clearcut within a decade before the 1980 eruption, and on three sites trees were knocked over by the lateral blast but remained on the hillslope (Table II). We also installed a stake array at the fringe of the blast-affected area where the forest had been singed but remained standing. This site was only measured in the first post-eruption year (Collins *et al.*, 1983; Collins, 1984).

We measured the exposed height of each stake relative to the tephra surface at the time of installation and on subsequent

Table II. Erosion study sites. For more details see Collins (1984) and Collins and Dunne (1986)

Site name (number in Figure 1)	Number of stakes ^a	Years of record	Hillslope gradient	Slope length (m)	Elevation (m)	Distance from volcano (km)	Land cover ^b
Coldwater 1 (5)	205 (152)	30	0.36	345	1100–1200	8.6	C
Coldwater 2 (6)	120 (63)	31	0.54	240	945–1095	8.9	D
Shultz 3 (3)	262 (182)	20	0.32	345	1010–1200	16.3	C, G
Maratta (4)	363 (152)	12	0.16	180	930–960	14.5	C, G
Shultz 1 (1)	376 (43)	12	0.25	625	710–890	17.6	C, G
Green 2 (10)	256 (144)	12	0.25	650	910–1010	17.7	C, G
Shultz 2 (2)	300 (188)	12	0.56	245	955–1025	16.6	C, G
Castle 1 (7)	298 (110)	12	0.66	645	930–1240	9.0	C
Green 1 (9)	210 (205)	2	0.25	725	915–1065	17.8	D
Castle 2 (8)	158 (158)	1	0.45	300	1045–1195	9.2	D

^aNumber of stakes installed in 1980; number in parentheses is the number of stakes measured at time of final measurement.

^bC = clearcut within 10 years prior to 1980 eruption; D = mature coniferous forest downed by 1980 eruption; S = standing forest singed by 1980 eruption; G = aerially seeded with grasses 4–5 months following the 1980 eruption.



Figure 2. The upslope portion of the Coldwater 1 erosion site, 1980–2010. (A) Rill networks in June 1980, a few weeks after the 18 May eruption. The silty airfall layer forms the surface of inter-rill areas. (B) In August 1983, the tephra surface had become coarser as the airfall layer had been locally stripped or had been coarsened by rainsplash and frost action. Rill edges had been rounded by rainsplash, frost action and animal trampling; larger rills had been partially filled by sediment and smaller rills had become indistinct from smoothing and filling. (C) By October 2010, as a result of the continued smoothing and filling of rills over the next decades, even the largest gullies were indistinct. Some sign of trampling by elk is visible in the foreground; while plant cover was low on much of the upper slope, cover was greater downslope where more tephra had eroded. [Colour figure can be viewed at wileyonlinelibrary.com]

visits. While making measurements, stakes were approached from downhill and care taken to avoid disturbing the surface near the stake or along transects; we did not observe upslope-propagating disturbances of the tephra surface resulting from our access. The two Coldwater sites were the longest monitored and also the most disturbed by animal trampling; when a stake was observed to be loose or bent over from trampling (or any other cause), we did not include its measurement. Excepting stakes disturbed by trampling or some other cause, stakes remained firmly anchored in the underlying soil and were not noticeably displaced from the vertical.

At each of six measurements made between September 1980 and May 1982 on eight sites, we sampled the bulk density of the upper 108 mm of the tephra to ensure that stake measurements were unaffected by compaction or turbation and detected no change over the first 2 years (Figure 4 of Collins and Dunne, 1986). Major and Yamakoshi (2005) report that by 2000, the highly turbated upper 25% of the lateral blast deposit on their infiltration plot, located within our Shultz 1 site, had a mean bulk density two-thirds that of an adjacent, unturbated sample. However, this site, which was at lower elevations (Table II) and had a thinner tephra layer than our other sites, had been densely afforested and artificially seeded with grasses, and we did not use it after 1992. While the possibility exists that turbation might have caused some inflation of the tephra on our sites, the tephra deposit at our two Coldwater sites, from which we have the longest record (Table II), was a sandy gravel, less densely packed than the fine and medium sand deposited at the Shultz Creek site, and we presume these coarser deposits would have been less subject to density changes.

At each measurement, we categorized the surface as ‘rilled’ or ‘unrilled’ and attributed change to the surface elevation between measurements according to the category at the time of the second measurement. At the first stake measurement, we averaged the local slope over a 0.3 m length centred at the stake. During each measurement we estimated plant cover using a 0.2×0.2 m string grid of 20 points centred at each stake (Collins and Dunne, 1988). We also measured the top width and average depth of all rills and gullies crossing each transect; rills became indistinct and were not measured after 1983. We expressed a net decrease in surface elevation (erosion) as positive and a net increase in surface elevation (deposition) as negative.

In 1992 we remeasured ~1200 stakes (of the ~2500 original stakes) on six sites that had survived, or partially survived, road building and logging. Two of three sites originally installed in downed forests had been destroyed by salvage logging. Five of the seven sites originally installed in pre-eruption clearcuts (Shultz 1, 2 and 3, Maratta and Green 2) were seeded with

grass in late 1980 (Collins and Dunne, 1988) and subsequently afforested. Afforested tree seedlings were small in 1992 but by 2000 had grown large enough that it became infeasible to measure stake heights or plant cover; hence, afforested sites were not measured after 1992. In 2000, we measured three sites (Shultz 3, Coldwater 1 and 2) and in 2010 two sites (Coldwater 1 and 2; Figure 1, Table II). During 1980–1983 we made separate measurements of cover by native and artificially seeded species, but in subsequent measurements we categorized cover as plant, plant litter or wood debris; detail on the recovery of vegetation on hillslopes covered by lateral blast deposits near Mount St. Helens can be found elsewhere (e.g. Halpern *et al.*, 1990; Lawrence and Ripple, 2000; Cook and Halpern, 2018).

Sites were originally selected in 1980 to represent the Toutle River basin’s range of hillslope gradients, forest cover types and tephra thicknesses, which facilitated calculating a basin-wide rate by characterizing the effects of these controlling variables on erosion rate and accounting for their distribution in the basin (Collins *et al.*, 1983). As the number of surviving sites dwindled, such a systematic estimate became impossible, and after 1983 basin-wide erosion was estimated by averaging erosion at the available sites in each period. Hillslope gradients of the sites measured during 1983–1992 average 0.39 (Table II), which is close to the 0.38 average of all hillslopes in the Toutle River portion of the blast-affected area (Collins *et al.*, 1983). However, the gradient of sites we measured in 2000 and 2010 averaged 0.41 and 0.45, respectively, biasing the sample towards steeper slopes in the latter two periods. More significantly, using our surviving sites to estimate basin-averaged erosion is limited by the absence of data on erosion from the large portion of the basin that had been reforested over that period; as a result, our estimates of basin-averaged erosion for 1992–2000 and 2000–2010 have large error bars.

To examine the possibility that variations in precipitation intensity within the 30-year period might have influenced erosion rates, we tabulated hourly precipitation records from the Cougar 4 SW gauge in four periods corresponding to our measurements, WY 1980–1983, WY 1984–1992, WY 1993–2000 and WY 2001–2010. Because the periods were of unequal length, we normalized the hourly precipitation frequencies by the number of years in each period.

Results

Erosion rates and processes

Elevation changes of inter-rill surfaces and rill beds in the 1983–1992 period were correlated with average hillslope

gradient in opposite ways (Figure 3A, Table III). Although the sample sizes are too small for formal statistical analysis, the measurements suggest that inter-rill erosion rates between 1.5 and 7.2 mm year⁻¹ continued to be positively correlated with gradient, while the rate of sedimentation in rills also increased with gradient from ~0 to 3.2 mm year⁻¹, suggesting that a portion of the intensified sediment supply from inter-rill surfaces was trapped in the rills as water infiltrated the beds (e.g.

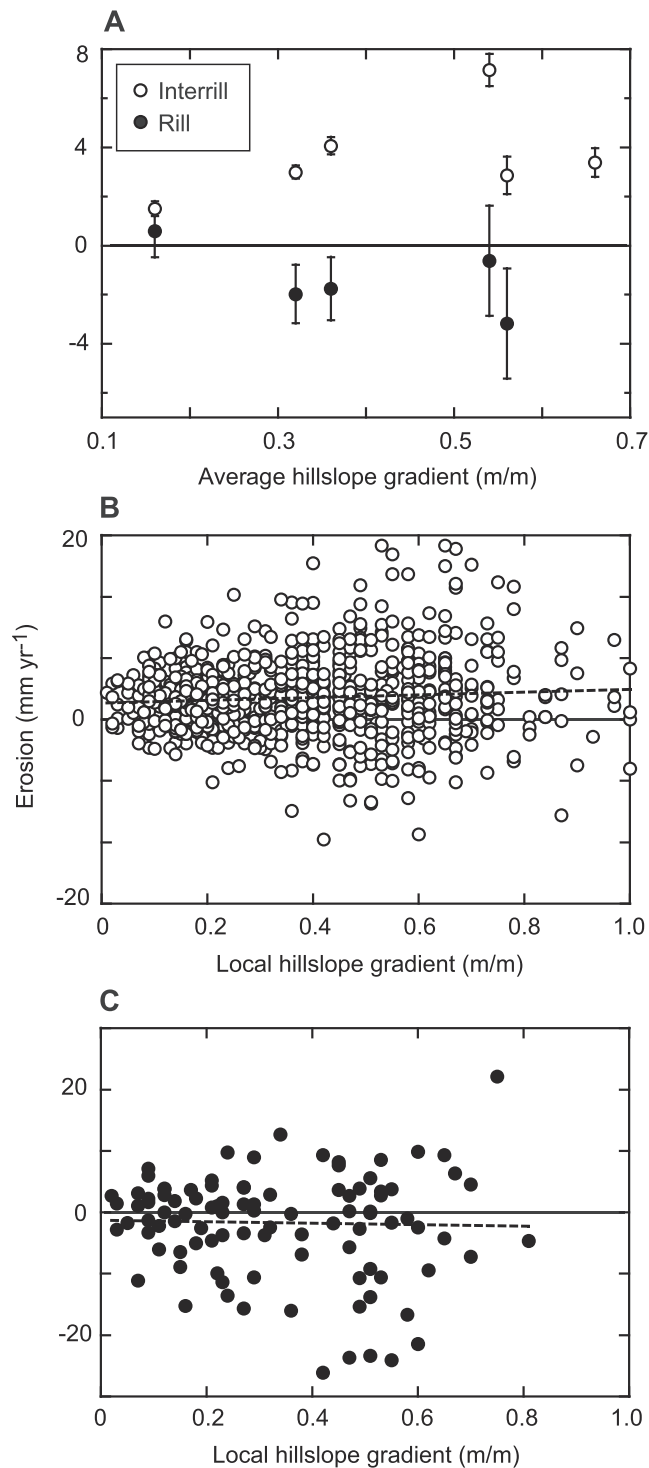


Figure 3. Erosion and deposition at stakes, 1983–1992. A positive value represents erosion and a negative value deposition. (A) Average annual erosion or deposition and average slope at eight sites with one standard error of the mean. (B) Average annual erosion or deposition from the same eight sites at stakes in surfaces identified in 1981/1983 as inter-rills. (C) Average annual erosion or deposition from the same eight sites at stakes in sites identified in 1981/1983 as rills.

Figure 2B). Only on the lowest gradient site, with a gradient of 0.16, did rill erosion continue in this period – presumably because the influx of sediment into rills from the intervening surfaces was relatively low but ephemeral flow continued to occur within the rills; on all steeper surfaces, rills aggraded. This filling of rills continued a trend that began in the second post-eruption year (Collins and Dunne, 1986). These measurements are consistent with visual observations of the increased sediment transport by rainsplash, frost action, dry ravel, animal burrowing and animal trampling.

Measurements at individual stakes indicate there was highly variable soil redistribution at the local scale (Figures 3B and C). Because we found no dependence of erosion rate on distance downslope, we combined stake measurements at all sites to characterize the local variability of erosion and the dependence of erosion rate on the local gradient (Figures 3B and C). The correlation between erosion and local gradient is consistent with the trend between site-averaged erosion and average hillslope gradient (Figure 3A). Erosion at individual stakes was only weakly correlated with gradient at the stakes on inter-rill surfaces (Figure 3B, Table IV) and local variability precluded recognizing a statistically significant trend in the smaller sample of stakes in rills (Figure 3C, Table IV). However, the weak trends that are indicated by the highly variable local measurements are consistent with the transect-averaged trends in Figure 3A.

Site-averaged net erosion from the six hillslopes monitored between 1983 and 1992 ranged from 1.4 to 5.9 mm year⁻¹ and roughly correlated with gradient (Figure 4B, Table III; for readability, the standard errors of the mean are omitted here and are reported in Table III). Annual net erosion from 1983 to 1992 averaged for all sites was 3.1 mm year⁻¹. The 1983–1992 average was only 7% of the average for 1980–1981 (45.6, or 47.2 mm year⁻¹, if the six sites that remained are considered), less than half that during 1981–1982 (6.5 mm year⁻¹) and statistically indistinguishable from the average of sites from 1982 to 1983 (3.8 mm year⁻¹).

After 1992, rills were too indistinct to separately identify stakes in rills, and we averaged elevation change at all stakes (Table III). Between 1992 and 2000, site-averaged elevation change, measured on three sites, ranged between -0.3 and 1.5 mm year⁻¹ (Figure 4B); only the latter value, from the steepest site, Coldwater 2, was significantly different from zero, and the average change from the three sites, 0.3 mm year⁻¹, was indistinguishable from zero (Table III). Between 2000 and 2010, changes at two remaining sites were -0.6 and 0.5 mm year⁻¹, but neither were significantly different from zero (Figure 4B, Table III). However, there was still considerable local sediment redistribution, with net annual average erosion or deposition of up to 10 mm at individual stakes, suggesting there was at least some downslope transport at rates below the resolution of our stake measurements indicated by the standard error of the means (Table III).

Role of revegetation

In the first few post-eruption years, vegetation cover (Figure 5A) remained generally low until after erosion rates had slowed (Figure 5B); vegetation cover was low in summer 1980 (range 0–1%; Figure 5A) and erosion was most rapid in the following rainy season (Figure 5B). Whereas in the first few post-eruption years the cover of vegetation increased modestly, nearly all plants, inclusive of native and artificially seeded species, grew in soil buried by the tephra and then exposed in rills and gullies, and erosion largely facilitated revegetation by exposing the underlying soil rather than being slowed by revegetation

Table III. Average erosion measured at erosion stakes for 1983–1992, 1992–2000 and 2000–2010, with one standard error, sample size *n* (number of stakes) and the probability in a one-tailed *t*-test that each mean value is different from zero. In the text, we accept any *p*-value < 0.05 as indicating elevation change. Erosion is expressed as a positive value, and deposition as a negative value

Site name	1983–1992						1992–2000		2000–2010	
	All	<i>n</i>	Inter-rill	<i>n</i>	Rill	<i>n</i>	All	<i>n</i>	All	<i>n</i>
Maratta	1.4 ± 0.3 <i>p</i> < 0.0001	155	1.5 ± 0.3 <i>p</i> < 0.0001	144	0.6 ± 1.1 <i>p</i> < 0.3	11				
Shultz 1 ^a	1.7 ± 0.7 <i>p</i> < 0.01	63	3.1 ± 1.1 <i>p</i> < 0.005	35	0.0 ± 0.6 <i>p</i> < 0.5	28				
Green 2 ^a	2.7 ± 0.6 <i>p</i> < 0.0001	144	4.2 ± 0.6 <i>p</i> < 0.0001	93	−0.1 ± 1.1 <i>p</i> < 0.5	51				
Shultz 3	2.5 ± 0.3 <i>p</i> < 0.0001	249	3.0 ± 0.3 <i>p</i> < 0.0001	223	−2.0 ± 1.2 <i>p</i> < 0.06	27	−0.3 ± 0.2 <i>p</i> < 0.10	177		
Coldwater 1	3.6 ± 0.4 <i>p</i> < 0.0001	189	4.1 ± 0.3 <i>p</i> < 0.0001	174	−1.8 ± 1.3 <i>p</i> < 0.10	15	−0.3 ± 0.4 <i>p</i> < 0.22	173	−0.6 ± 0.4 <i>p</i> < 0.07	138
Coldwater 2 ^b	5.9 ± 0.7 <i>p</i> < 0.0001	81	7.2 ± 0.7 <i>p</i> < 0.0001	68	−0.6 ± 2.2 <i>p</i> < 0.4	13	1.5 ± 0.6 <i>p</i> < 0.006	74	0.5 ± 0.7 <i>p</i> < 0.25	38
Shultz 2	1.8 ± 0.8 <i>p</i> < 0.012	184	2.9 ± 0.8 <i>p</i> < 0.0002	150	−3.2 ± 2.2 <i>p</i> < 0.08	34				
Castle 1	3.4 ± 0.6 <i>p</i> < 0.0001	158	3.4 ± 0.6 <i>p</i> < 0.0001							
All sites ^a	3.1 ± 0.8 <i>p</i> < 0.006	6	3.7 ± 0.9 <i>p</i> < 0.004	6	−1.4 ± 0.7 <i>p</i> < 0.05	5	0.3 ± 0.6 <i>p</i> < 0.35	3	−0.0 ± 0.6 <i>p</i> < 0.48	2
All stakes ^a	3.0 ± 0.2 <i>p</i> < 0.0001	967	3.5 ± 0.2 <i>p</i> < 0.0001	870	−1.7 ± 0.9 <i>p</i> < 0.03	99	0.0 ± 0.2 <i>p</i> < 0.50	427	−0.4 ± 0.4 <i>p</i> < 0.09	177

^aThe Shultz 1 and Green 2 sites were measured in 1981 and 1992. Because the sites were not measured in 1983, the values are reported in this table but have been excluded from the analysis.

^bWe measured the Coldwater 1 site in 2010 and Coldwater 2 in 2011; for simplicity, the two measurements are referred to herein as a 2010 measurement.

Table IV. Regression equations for average annual erosion at individual stakes, 1983–1992

Time period	Variable	Regression equation					Measured and predicted values		
		y (erosion, mm year ^{−1}) = $ax + b$					Measured <i>x</i> values	Predicted <i>y</i> at min <i>x</i> (mm)	Predicted <i>y</i> at max <i>x</i> (mm)
		<i>a</i>	<i>b</i>	<i>R</i> ²	<i>n</i>	<i>p</i>			
1983–1992	Site-avg. slope	4.0	1.4	0.21	6	0.36	0.16–0.66	2.0	4.0
	Site-avg. slope (inter-rill)	4.9	1.5	0.23	6	0.33	0.16–0.66	2.3	4.8
	Site-avg. slope (rill)	−5.4	0.7	0.39	5	0.26	0.16–0.56	−0.2	−2.3
	Local slope	2.3	2.1	0.01	965	0.02	0.01–1.73	2.1	6.2
	Local slope (inter-rill)	2.3	2.6	0.007	867	0.01	0.01–1.73	2.7	6.6
	Local slope (rill)	−1.2	−1.3	0.001	99	0.80	0.02–0.81	−1.3	−2.2
	Vegetative cover	−0.040	4.8	0.05	966	<0.0001	0–100	4.8	0.8
1992–2000	Local slope	0.41	−0.13	0.0002	427	0.76	0.02–0.84	−0.1	0.21
	Vegetative cover	−0.026	1.4	0.05	414	<0.0001	0–100	1.4	−1.1
2000–2010	Local slope	4.6	−2.2	0.02	176	0.09	0.07–0.84	−1.8	1.7
	Vegetative cover	0.0016	−0.44	0.0001	174	0.89	0–100	−0.4	−0.3

Note: ‘Vegetative cover’ is the total percentage cover measured in a 0.2 × 0.2 m grid at each stake (see Collins and Dunne, 1988 for details) and includes live and dead vegetation and litter. Erosion is expressed as a positive value, and deposition as a negative value.

(Collins and Dunne, 1986). The plant cover at the Shultz 1 site (Figure 5A) responded faster than at other locations because it was the most effectively seeded site, and because the relative thinness of the original tephra layer facilitated exposure of buried soil by rills and gullies (Collins and Dunne, 1988). Vegetation cover remained low in 1983 on other sites (Figure 5A).

Between 1983 and 1992, the total ground cover provided by plants, plant litter and exhumed wood debris increased substantially (Figure 5A, Table V) as erosion continued to expose the buried soil and as erosional stripping of the fine surficial tephra and accumulation of litter created a more favourable environment on the tephra surface. In summer 1983, the cover of plants and litter (excluding wood debris; Table V) ranged from 16 to 66% on five seeded sites and 6 to 21% on three unseeded

sites. In 1992, on the same sites, there was less difference in cover between the seeded (41–72%) and unseeded (39–41%) sites, and qualitatively we observed that most of the cover provided by seeded plants was litter. Planted conifers were small in 1992 and contributed minor cover except at the Green River 2 (GR2) site, where they attained a height of 3–5 m and provided much of the cover (19% cover by afforested trees and 22% cover from other plants). Total plant cover on three sites in 2000 ranged from 51 to 63% and on two sites in 2010 was 49 and 68%. On average, wood debris provided an additional 5 to 8% of cover in the three periods (Table V).

As vegetative cover increased after the first few post-eruption years, and as rainsplash and bioturbation became the dominant erosion processes, vegetation began to influence erosion.

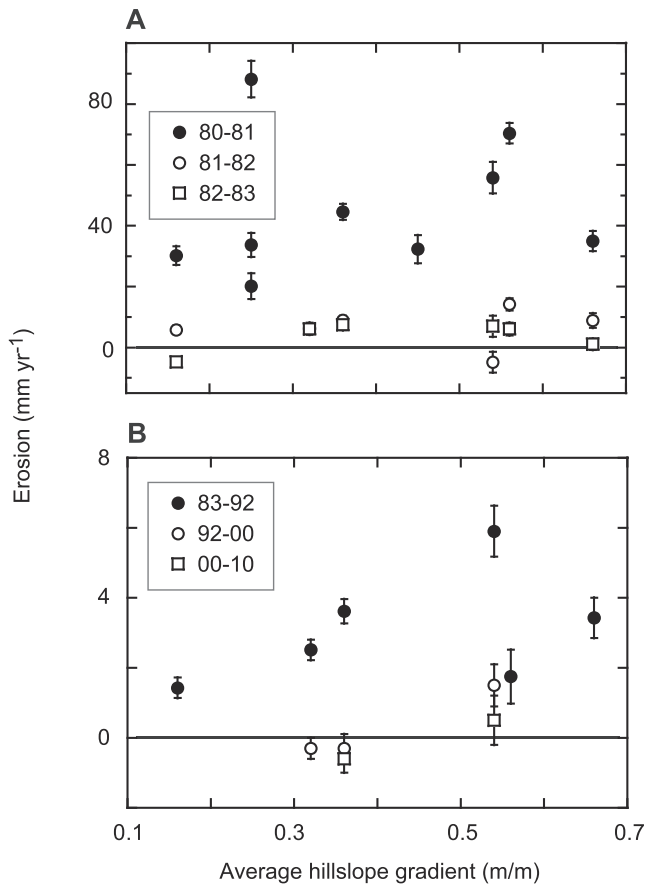


Figure 4. Site-averaged net erosion, with one standard error of the mean and average hillslope gradient: (A) 1980–1981, 1981–1982 and 1982–1983 (from Collins, 1984); (B) 1983–1992, 1992–2000 and 2000–2010. Note the change in ordinate scale between the panels.

Erosion at individual stakes weakly but significantly correlated inversely with plant and litter cover (Figure 6, Table IV). Linear regression of erosion measured at individual stakes and local plant cover predicts for the 1983–1992 period an erosion rate of 4.6 mm year^{-1} at 0% cover and 0.7 mm year^{-1} at 100% cover (Figure 6A, Table IV); the same regression for the 1992–2000 period indicates that, on average, erosion occurred only on surfaces having less than about 54% cover (Figure 6B, Table IV). There was no correlation between erosion and vegetation cover in the 2000–2010 period (Table IV).

Effects of variation in storm intensity during the three-decade period

The 2-year, 1-h intensity of 14 mm h^{-1} from the 32-year record at the Cougar 4 SW station is close to the 16.5 mm h^{-1} estimated by Miller *et al.* (1973) for our sites. While the frequency of precipitation intensities $<10 \text{ mm h}^{-1}$ at the Cougar 4 SW gauge was consistent between the four periods of erosion measurement, there was greater between-period variation for higher-intensity events. WY 1984–1992, with about 5 h of rainfall intensities $>10 \text{ mm h}^{-1}$, had the most hours of higher-intensity rainfall. Comparison of rainfall intensities and infiltration rates predicts that overland flow would have occurred on bare tephra about 10 to several hundred hours per year in 1980 and 1981, but only ~ 0.1 to $<10 \text{ h year}^{-1}$ by the year 2000 (Figure 7); the absence of infiltration measurements between 1981 and 2000 makes it impossible to estimate the frequency of runoff events in the WY 1984–1992 period, which

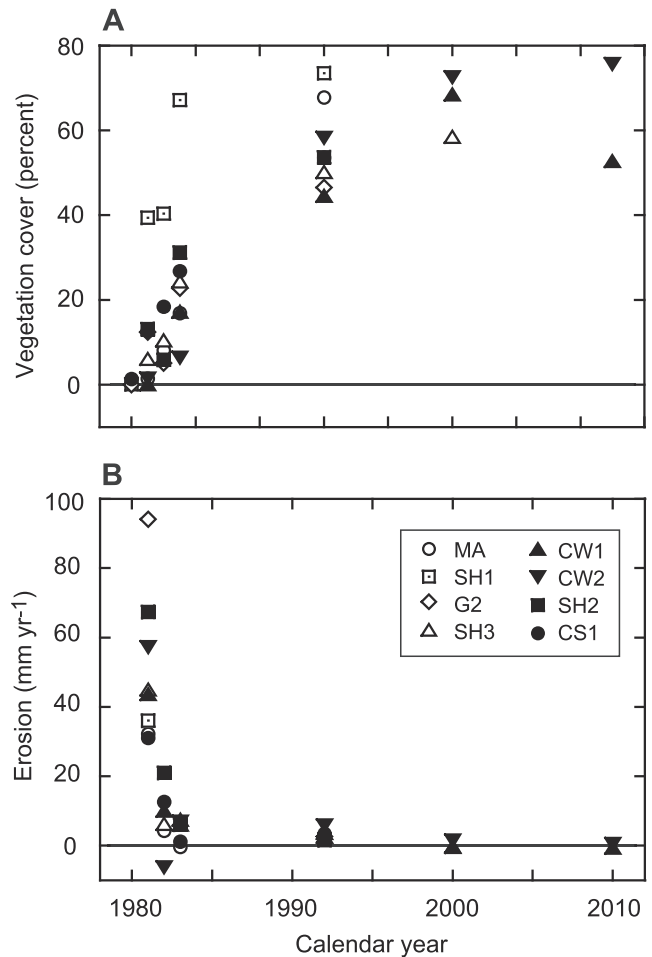


Figure 5. (A) Mean cover of plants, litter and wood fragments, 1980–2010. (B) average annual erosion, 1980–2010. Solid symbols indicate monitored hillslopes from Table I: MA = Maratta; SH1 = Schultz 1; GR2 = Green 2; SH3 = Shultz 3; CW1 = Coldwater 1; CW2 = Coldwater 2; CS1 = Castle 1.

had higher-intensity storms. The actual number of hours of precipitation-generated overland flow is probably less than indicated by these predictions, especially at the higher-elevation sites, because of the persistence of winter snow cover (see earlier). There are no data on infiltration rates in the third post-eruption decade following the Major and Yamakoshi (2005) study, but there is no reason to expect that infiltration capacity would have decreased.

Contribution of tephra erosion to volcanogenic sediment yield

Basin-wide hillslope erosion declined throughout the first 20 post-eruption years (Figure 8A); rates for the 1992–2000 and 2000–2010 periods are statistically indistinguishable from zero, and the rate for the third post-eruption decade equalled zero (Table III). Exponential and power curves fit the data about equally, and moderately, well; because neither is informative about the physical processes causing the decline in erosion rate, we show the exponential fit (Figure 8A) to facilitate comparison with other studies because an exponential is commonly used to characterize relaxation times of fluvial systems, including sediment yield following volcanic eruptions (e.g. Gran *et al.*, 2011).

Annual suspended sediment flux from the Green River basin, measured by the US Geological Survey (Major *et al.*, 2000), also declined on average in the 14-year period (WY 1982–

Table V. Vegetative cover averaged for all stakes measured at each site in 1983, 1992, 2000 and 2010. In 1983, cover by plants is divided into native and seeded species, and litter is also divided into that provided by native and seeded species. At subsequent measurements total cover was simply divided into plant cover and litter

Site	1983					1992			2000			2010		
	Plant cover (%)		Litter (%)		Wood	Plant cover (%)	Litter (%)	Wood	Plant cover (%)	Litter (%)	Wood	Plant cover (%)	Litter (%)	Wood
	N	S	N	S										
Maratta	9.6	6.2	0.4	0.7	0.0	38.0	24.1	5.8						
Shultz 1	38.5	18.1	5.3	3.6	1.7	52.0	19.8	1.7						
Green 2	1.9	9.6	0.3	0.0	6.7	40.2	0.7	5.5						
Shultz 3	14.0	0.2	2.4	0.0	7.8	27.6	14.1	8.5	42.5	8.2	7.9			
Coldwater 1 ^a	9.9	NS	0.2	NS	7.2	30.1	8.8	5.8	47.2	15.9	5.4	39.1	10.1	3.6
Coldwater 2 ^a	6.3	NS	0.0	NS	0.0	32.5	8.7	16.9	49.9	12.6	10.0	59.6	8.4	7.6
Shultz 2	16.3	2.4	3.7	0.0	8.8	29.2	18.6	5.9						
Castle 1	19.2	NS	1.8	NS	5.8	28.8	10.6	14.3						

^aAverage plant cover at the Coldwater sites in 2010 is an underestimate because ground cover could not be measured reliably at six stakes in dense scrub-shrub thickets.

Note: N indicates native species and S artificially seeded species and planted conifers. NS indicates site was not seeded. 'Wood' is woody material on the buried soil exposed by erosion or tree fragments incorporated in the original blast deposit.

1994) it was measured (Figure 8B). The 339 km² drainage area above the Green River gauging station (Figure 1) includes tephra-covered hillslopes but does not include debris avalanche, pyroclastic flow or debris flow deposits, and is thus a good indicator of erosion of the lateral blast deposits (Major

et al., 2000). Spatially averaged suspended-sediment yields for the entire Green River basin were initially much lower than hillslope-averaged tephra erosion rates. For example, the second post-eruption year's hillslope erosion rate of 7 mm year⁻¹

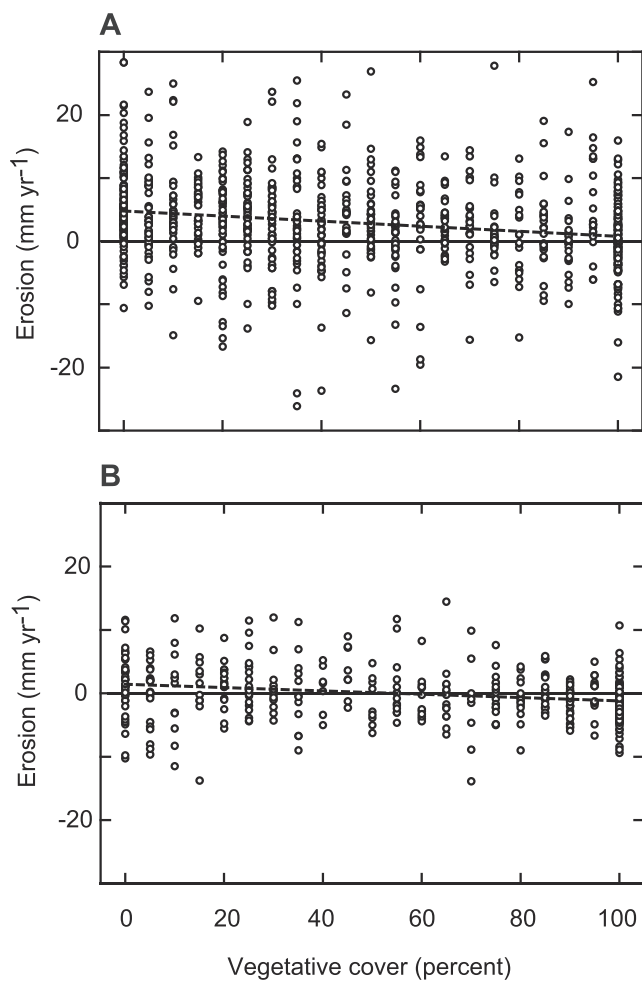


Figure 6. Elevation change at individual stakes related to vegetative ground cover: (A) erosion 1983–1992 and vegetation cover in 1992; (B) erosion 1992–2000 and vegetation cover in 2000. Statistics for the regressions, and for regressions of the 2000–2010 data, are listed in Table III.

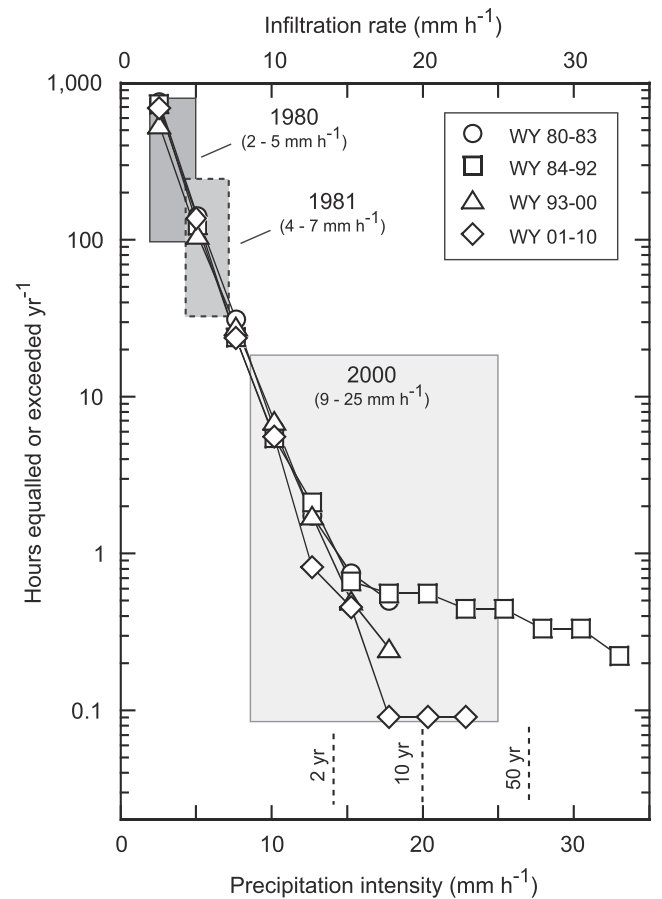


Figure 7. Magnitude and frequency of hourly precipitation recorded at the Cougar 4 SW gauge, located 30 km SSW of the Coldwater sites (Figure 1). Data are presented separately for each of four time periods bracketing erosion measurements. Dashed vertical lines indicate the predicted magnitude of the 1-h precipitation event having 2, 10 and 50-year recurrence, as determined from Miller *et al.* (1973). Shaded areas represent the infiltration rates measured in two studies on our Shultz Creek site in 1980 and 1981 (Leavesley *et al.*, 1989) and in 2000 (Major and Yamakoshi, 2005).

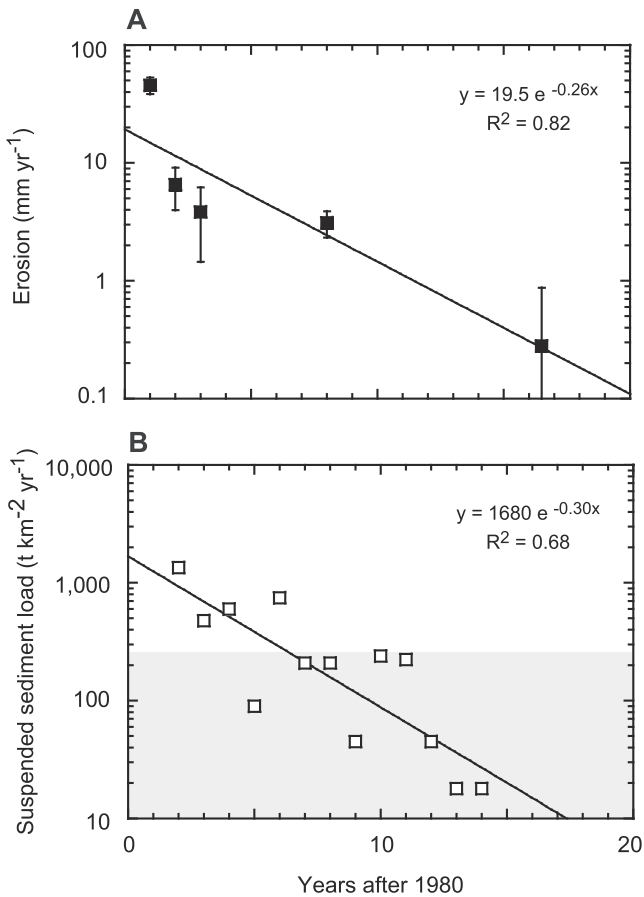


Figure 8. (A) Change through time in average annual erosion averaged from all sites measured in summer 1980–1981, 1981–1982, 1982–1983, 1983–1992 and 1992–2000 fitted to an exponential function. Equation for data fit to power function (not shown) is $y = 31.1x^{-1.54}$, $R^2 = 0.89$, $p = 0.007$. (B) Annual suspended sediment transport at the USGS Green River gauge (Figure 1), WY 1982–1994, from Major *et al.* (2000) fitted to an exponential function. Equation for data fit to power function (not shown) is $y = 5600x^{-1.84}$, $R^2 = 0.62$, $p = 0.001$. Shaded area represents range of sediment loads in regional rivers reported for unglaciated rivers in the Cascade Range of southwestern Washington and northwestern Oregon.

translates to a sediment supply rate of $7000 \text{ t km}^{-2} \text{ year}^{-1}$ for a soil of density 1000 kg m^{-3} , several times higher than the basin-wide sediment yield for that year (Figure 8B). This discrepancy is presumably because erosion rates from our study sites only apply to a portion of the basin, which also includes forests singed by the eruption and undisturbed forest, where the infiltration capacity remained high and erosion was not accelerated by the eruption, as well as salvage-logged and replanted hillslopes within the blast-affected area, where mechanical disturbance increased infiltration and detention of runoff and decreased erodibility (Collins and Dunne, 1988). A likely smaller, countervailing effect is that the sediment transported as bedload is unaccounted for, and bedload averaged 18% of the total load measured in November 1980–February 1981 in four Toutle River tributaries by Lehre *et al.* (1983). The discrepancy is not likely caused by storage of eroded tephra in the drainage network: repeated cross-sectional surveys in several tributaries to the Toutle River system in 1980–1981 showed a net export of channel sediments (Lehre *et al.*, 1983) and channels in the Clearwater Creek drainage generally incised within the first 5 years after the eruption (Lisle, 1995). For these reasons it is not possible to directly compare the absolute rates of tephra erosion and suspended sediment yield, but both slowed at a similar rate; the e-folding rates in the exponential equations

are -0.26 year^{-1} for erosion and -0.30 year^{-1} for sediment yield.

Within about 6 years after the 1980 eruption, the catchment-scale sediment flux dropped into the range of $10\text{--}250 \text{ t km}^{-2} \text{ year}^{-1}$ (assuming a soil bulk density of 1000 kg m^{-3} , this is equivalent to hillslope lowering rates of $0.01\text{--}0.25 \text{ mm year}^{-1}$). These rates are within the range of suspended sediment yields measured from forested watersheds lacking active glaciers in the Cascade Range of southwestern Washington and northwestern Oregon (Czuba *et al.*, 2011; Wise and O'Connor, 2016; Bywater-Reyes *et al.*, 2018), and is similar to the conclusion of Major *et al.* (2018) that sediment yield from the Green River basin declined to pre-eruption levels within about 5 years. By that time, tephra erosion rates were approaching the limits of measurement (Figure 8A, Table III), suggesting that the contribution of tephra erosion to streams had declined to the background level of the surrounding undisturbed landscape and that the 1980 tephra had entered the sediment supply system driven by fast and slow mass wasting.

Discussion

Evolution of erosion processes through time

What did extending the field experiment for three decades reveal about erosion processes beyond what had been learned from the first 3 years of observations? The first 3 years of observations showed that a stable network of rills developed as rills rapidly extended to within centimetres of local drainage divides. The rill formation intensified erosion rates both by direct evacuation of the channel volumes and by facilitating the export of inter-rill sediment, which might otherwise be redeposited downslopes. Then, as the network developed in the first several post-eruption months, rill densities declined rapidly as the size of rills increased (Collins and Dunne, 1986) and smaller rills were subject to cross-grading (development of a lateral component of gradient and flow towards master rills) and micro-piracy (Horton, 1945). In field experiments, rainsplash is typically important in detaching sediment, which sheetwash transports more efficiently (e.g. Morgan, 1978; Ghahramani *et al.*, 2011), and an equilibrium develops between the two processes as a stable rill network establishes (Dunne and Aubry, 1986). In the first few years of observations, the smoothing of smaller rills (Collins and Dunne, 1986), the accumulation in rills of sediment eroded from inter-rill areas (Figure 5 of Collins and Dunne, 1986; Dunne and Aubry, 1986) and the degradation of rill edges (e.g. Figure 2B) all suggested that the intensity of sheetwash erosion began to give way in the first post-eruption year to rainsplash, frost action and bioturbation in transporting sediment, a shift interpreted from visual observations to have resulted from physical changes to the tephra surface that affected surface runoff and erodibility.

Extended monitoring over the next three decades showed the effects of the continued shift in dominance to diffusive processes. This continued shift was driven by an increase in tephra infiltration capacity (Leavesley *et al.*, 1989; Major and Yamakoshi, 2005), presumably because frost action and bioturbation disrupted the fine-grained surface layer and erosion stripped that layer and exposed underlying coarser tephra, and because a coarsened surface and coarser underlying layers had lower cohesion and less resistance to rainsplash detachment (Dunne *et al.*, 2010). Additionally, runoff generated on the inter-rill surface would infiltrate into rill beds cut into the coarser sands of the lower strata of the surge deposit and the underlying soil exposed in rill beds, causing rills to trap

material splashed and washed from inter-rill surfaces. The result of the continued shift towards diffusive processes was the continued smoothing of rill channels during 1983–1992 to the extent that few rills were identifiable in the landscape by 2000 (e.g. Figure 2C).

Not apparent from the first few years of this study (or in reports from other short-term tephra erosion studies) was the importance of animals both in transporting sediment downslope and in mixing tephra layers and thus indirectly contributing to the increased role of rainsplash. Evidence of trampling by Roosevelt elk (*Cervus elaphus roosevelti*) was widespread on the two Coldwater sites. In areas of chronic, concentrated elk traffic, trampling appears to retard or prevent revegetation and to transport tephra downslope. In contrast, trampling also mixes the coarser lower strata with finer upper strata, which increases infiltration and could decrease erodibility. Burrowing by small mammals was also observed to be widespread and to result in both downslope transport and mixing of tephra.

While shorter-term studies have shown that erosion began to slow prior to widespread revegetation, this longer-term study shows that physical changes, even in areas lacking any vegetation cover, can slow erosion below levels detectable by our measurement methods. Re-established vegetation remained patchy through 1992, but erosion was reduced in proportion to its presence. Broad spatial patterns of plant recovery on our sites are consistent with those revealed by remotely sensed cover throughout the entire blast-affected area by Lawrence and Ripple (2000): our sites farther from the volcano generally had greater cover, reflecting the favourable effect of thinner tephra on plant recovery, as did our sites on steeper slopes, reflecting the favourable effects of erosional stripping of tephra. Erosion during 1992–2000 was either small or indistinguishable from zero ($0.3 \pm 1.0 \text{ mm year}^{-1}$), and in any case had dropped below measurable rates by 2000–2010 ($0.0 \pm 0.6 \text{ mm year}^{-1}$). Though vegetation cover increased, the surface on many sites remained sparsely vegetated, and yet erosion effectively ceased even in the absence of local revegetation.

Finally, extending the field experiment over several decades shows that the deposits' rapid stabilization appears to be a relatively robust phenomenon; the stabilization continued even with unusually high-intensity precipitation events during 1983–1992 (Figure 7). Infiltration capacities of Mount St. Helens tephra and precipitation intensities are low compared to those from other volcanoes (Table 1 and Figure 4 of Pierson and Major, 2014). However, physical stabilization of the tephra surface has been reported for tephra having a variety of grain sizes and subject to a variety of precipitation intensities (e.g. Segerstrom, 1960; Waldron, 1967; Ollier and Brown, 1971; Kadomura *et al.*, 1983; Yamamoto, 1984; Chinen, 1986; Shimokawa and Jitousono, 1987; Miyabuchi *et al.*, 1999). In each case, the disturbed surface was initially dissected by channels of various sizes, the spacing of which reduced runoff paths below a critical value for erosion (Horton, 1945); the long-term shift in dominance from incisive to diffusive processes documented in this study then also played a role in altering the channel spacing.

Fate of tephra on hillslopes

Visual observations indicate that on slopes steeper than about 0.7, similar to observations made at other volcanoes (see earlier), erosion stripped most or all of the tephra layer in the first few years. But our results suggest that on moderate to gentle hillslopes with moderate to thick tephra, much of an erupted tephra will remain on hillslopes, at least for some time, whether or not revegetation occurs soon after an eruption. This confirms

the inference, made from short-term studies at Mount St. Helens and Usu volcanoes (Kadomura *et al.*, 1983; Collins and Dunne, 1986; Smith and Swanson, 1987), that the largest portion of tephra will become buried with plant litter, incorporated into soil horizons and accommodated, over the long term (10^2 – 10^4 years), by an increase in soil depth and soil creep transport rate (Heimsath *et al.*, 2005).

Various flora and fauna are effective soil mixing agents (for a review, see e.g. Gabet *et al.*, 2003), and the tendency through time for a tephra layer to homogenize or remain as a distinct horizon will vary generally with the mixing agents present in a given environment (Blong *et al.*, 2017). For example, in some parts of the area affected by the lateral blast at Mount St. Helens, the northern pocket gopher (*Thomomys talpoides*) brought buried soil to the tephra surface starting in the first few months following the eruption (Andersen and MacMahon, 1985). Preservation through time of deposits from the Mount St. Helens lateral blast, and tephra layers generally, as distinct layers, requires that a tephra layer be thicker than the sum of the depths of short-term erosion and the bioturbation zone, or the entire eruption layer will be disrupted and creep downslope. Also, the frequency and magnitude of tephra depositional events over time must exceed the sum of surface erosion and creep between eruptions. Lack of erosional contacts in a tephra sequence implies that eruptions must be very frequent. Expanding the records of these processes makes such quantification possible.

The role of tephra in sediment yields following volcanic eruptions

The current conceptual model of erosion following volcanic eruptions is that hillslope tephra erosion is a short-term (several-year) sediment source, and that fluvial channel network development and channel widening in valley-filling debris avalanche, pyroclastic flow and mudflow deposits result in a longer-term sediment supply (Manville *et al.*, 2009; Gran *et al.*, 2011; Pierson and Major, 2014). This model has been developed from studying fluvial erosion of valley-filling deposits, most intensively at Mt. Pinatubo (e.g. Pierson *et al.*, 1992; Scott *et al.*, 1996; Montgomery *et al.*, 1999; Hayes *et al.*, 2002; Gran and Montgomery, 2005; Gran *et al.*, 2011) and Mount St. Helens (e.g. Lehre *et al.*, 1983; Meyer and Martinson, 1989; Simon, 1999; Major *et al.*, 2000, 2018; Major, 2004; Zheng *et al.*, 2014), as well as volcanoes in central America (e.g. Kuenzi *et al.*, 1979; Inbar *et al.*, 1994), Indonesia (e.g. Lavigne, 2004) and New Zealand (e.g. Manville *et al.*, 2009), combined with inference from short-term tephra erosion studies and suspended sediment studies (e.g. Major, 2004). This study confirms the inference that the contribution of hillslope tephra erosion to basin sediment yield, at least in a temperate environment, is likely to be large for only several years, with the erosion after that point appearing to be slow and likely contributing little sediment directly to channels. At Mount St. Helens, this stabilization benefitted from, but happened even in the absence of, revegetation, and was largely due to changes in dominant sediment transport process – from sheetwash and rilling to rainsplash and rill sedimentation – and changes to the physical and hydrologic properties of the tephra.

Conclusions

While in the first few post-eruption years sheetwash and rill erosion were the dominant processes eroding tephra deposited by the May 1980 eruption of Mount St. Helens, within the first

few post-eruption months process dominance began to shift to diffusive processes as rainsplash, frost action, bioturbation and erosional stripping of the low-infiltration surface layer increased infiltration and reduced erodibility, smoothing and erasing rills that had formed on hillslopes within the first few post-eruption years, eventually erasing rills altogether. Even on unvegetated surfaces, erosion rates within 12 years after the eruption had diminished to below levels detectable by our measurement methods, even during a period of relatively intense rainfall, as the same physical processes that had earlier stabilized surfaces with respect to sheetwash and rill erosion in the first few post-eruption years stabilized surfaces relative to rainsplash. As a result, tephra erosion was a transient contributor to the post-eruption sediment budget of rivers draining the north side of the volcano: watershed-scale suspended sediment measurements suggest that contributions of sediment from hillslopes to streams had ceased as early as 6 years after the eruption. The short-term nature of the sediment source is consistent with predictions made from measurements of erosion in the first three post-eruption years, and confirms the current conceptual model of the role played by tephra erosion relative to other sediment sources following volcanic eruptions. While tephra deposited on the steepest slopes has been stripped by erosion, as a result of erosional stabilization of tephra on moderate and gentle slopes, 30 years after its deposition most of the tephra deposited on such hillslopes remains in place. The extent to which tephra will be preserved as a distinct layer will likely depend on the balance between these mixing and redistributing agents versus revegetation and soil formation on the tephra surface.

Acknowledgements—We thank John Costa of the U.S. Geological Survey Cascades Volcano Observatory for logistical support for the 1992 field measurements; David Montgomery, Erin Pettit and Vivian Leung for their assistance with field measurements in 2000 and 2010; and Jon Major and Alan Palmer for their helpful reviews.

References

- Andersen D, MacMahon J. 1985. Plant succession following the Mount St. Helens volcanic eruption: facilitation by a burrowing rodent, *Thomomys talpoides*. *The American Midland Naturalist* **114**: 62–69. <https://doi.org/10.2307/2425241>.
- Blong R, Enright N, Grasso P. 2017. Preservation of thin tephra. *Journal of Applied Volcanology* **6**: 10. <https://doi.org/10.1186/s13617-017-0059-4>.
- Bywater-Reyes S, Bladon KD, Segura C. 2018. Relative influence of landscape variables and discharge on suspended sediment yields in temperate mountain catchments. *Water Resources Research* **54**: 5126–5142. <https://doi.org/10.1029/2017WR021728>.
- Chinen T. 1986. Surface erosion associated with tephra deposition on Mt. Usu and other volcanoes. *Environmental Science, Hokkaido: Journal of the Graduate School of Environmental Science, Hokkaido University, Sapporo* **9**: 137–149.
- Chinen T, Kadamura H. 1986. Post-eruption sediment budget of a small catchment on Mt. Usu, Hokkaido. *Zeitschrift für Geomorphologie* **60**: 217–232.
- Chinen T, Riviere A. 1990. Post-eruption erosion processes and plant recovery in the summit atrio of Mt. Usu, Japan. *Catena* **17**: 305–314. [https://doi.org/10.1016/0341-8162\(90\)90023-7](https://doi.org/10.1016/0341-8162(90)90023-7).
- Collins BD. 1984. Erosion of tephra from the 1980 eruption of Mount St. Helens. Thesis, University of Washington, Seattle, WA.
- Collins BD, Dunne T. 1986. Erosion of tephra from the 1980 eruption of Mount St. Helens. *Geological Society of America Bulletin* **97**: 896–905. [https://doi.org/10.1130/0016-7606\(1986\)97<896:EOTFTE>2.0.CO;2](https://doi.org/10.1130/0016-7606(1986)97<896:EOTFTE>2.0.CO;2).
- Collins BD, Dunne T. 1988. Effects of forest land management on erosion and revegetation after the eruption of Mount St. Helens. *Earth Surface Processes and Landforms* **13**: 193–205. <https://doi.org/10.1002/esp.3290130302>.
- Collins BD, Dunne T, Lehre AK. 1983. Erosion of tephra-covered hillslopes north of Mount St. Helens, Washington: May 1980–May 1981. *Zeitschrift für Geomorphologie Supplement* **46**: 103–121.
- Cook JE, Halpern CB. 2018. Vegetation changes in blown-down and scorched forests 10–26 years after the eruption of Mount St. Helens, Washington, USA. *Plant Ecology* **219**: 957–972. <https://doi.org/10.1007/s11258-018-0849-8>.
- Crisafulli CM, Dale VH. 2018. Ecological responses to the 1980 eruption of Mount St. Helens: key lessons and remaining questions. In *Ecological Responses at Mount St. Helens: Revisited 35 Years After the 1980 Eruption*, Crisafulli CM, Dale VH (eds). Springer: New York; 1–18.
- Czuba JA, Magirl CS, Czuba CR, Grossman EE, Curran CA, Gendaszek AS, Dinicola RS. 2011. *Sediment load from major rivers into Puget Sound and its adjacent waters*, US Geological Survey Fact Sheet 2011-3083. US Geological Survey: Reston, VA.
- del Moral R, Grishin SY. 1999. Volcanic disturbances and ecosystem recovery. In *Ecosystems of Disturbed Ground*, Walker LR (ed). Elsevier: Amsterdam; 137–160.
- Dunne T, Aubry BF. 1986. Evaluation of Horton's theory of sheetwash and rill erosion on the basis of field experiments. In *Hillslope Processes*, Abrahams AD (ed). George Allen & Unwin: London; 31–53.
- Dunne T, Malmon DV, Mudd SM. 2010. A rainsplash transport equation assimilating field and laboratory measurements. *Journal of Geophysical Research – Earth Surface* **115**: F01001. <https://doi.org/10.1029/2009JF001302>.
- Eggler WA. 1959. Manner of invasion of volcanic deposits by plants, with further reference from Paricutin and Jerullo. *Ecological Monographs* **29**: 267–284. <https://doi.org/10.2307/1942281>.
- Eggler WA. 1963. Plant life of Paricutin Volcano, Mexico, eight years after activity ceased. *The American Midland Naturalist* **69**: 38–68. <https://doi.org/10.2307/2422843>.
- Fairchild LH. 1987. The importance of lahar initiation processes. *Reviews in Engineering Geology* **7**: 51–62. <https://doi.org/10.1130/REG7-p51>.
- Franklin JF, Dyrness CT. 1973. *Natural Vegetation of Oregon and Washington*. USDA Forest Service General Technical Report PNW-8; 417 pp.
- Gabet EJ, Reichman OJ, Seabloom EW. 2003. The effects of bioturbation on soil processes and sediment transport. *Annual Review of Earth and Planetary Sciences* **31**: 249–273. <https://doi.org/10.1146/annurev.earth.31.100901.141314>.
- Ghahramani A, Ishikawa Y, Gomi T, Miyata S. 2011. Downslope soil detachment – transport on steep slopes via rain splash. *Hydrological Processes* **25**: 2471–2480. <https://doi.org/10.1002/hyp.8086>.
- Gil-Solórzano D, Sabina Lara-Cabrera S, Lindig-Cisneros R. 2009. Effects of organic matter added to sand deposits of volcanic origin on recruitment of seedlings. *The Southwestern Naturalist* **54**: 439–445. <https://doi.org/10.1894/DW-120.1>.
- Glicken HX. 1996. *Rockslide-debris Avalanche of May 18, 1980, Mount St. Helens Volcano, Washington*, US Geological Survey Open-File Report 96-677. US Geological Survey: Reston, VA.
- Gran KB, Montgomery DR. 2005. Spatial and temporal patterns in fluvial recovery following volcanic eruptions: channel response to basin-wide sediment loading at Mount Pinatubo, Philippines. *Geological Society of America Bulletin* **117**: 195–211. <https://doi.org/10.1130/B25528.1>.
- Gran KB, Montgomery DR, Halbur JC. 2011. Long-term elevated post-eruption sedimentation at Mount Pinatubo, Philippines. *Geology* **39**: 367–370. <https://doi.org/10.1130/G31682.1>.
- Griggs RF. 1918. The recovery of vegetation at Kodiak. *Ohio Journal of Science* **19**: 1–57. <http://hdl.handle.net/1811/2010>.
- Griggs RF. 1919a. The character of the eruption as indicated by its effects on nearby vegetation. *Ohio Journal of Science* **19**: 173–209. Available at. <http://hdl.handle.net/1811/2020>.
- Griggs RF. 1919b. The beginnings of revegetation in Katmai valley. *Ohio Journal of Science* **9**: 318–342. Available at. <http://hdl.handle.net/1811/2040>.
- Grishin SY, del Moral R, Krestov PV, Verkholat VP. 1996. Succession following the catastrophic eruption of Ksudach Volcano (Kamchatka, 1907). *Vegetatio* **127**: 129–153. www.jstor.org/stable/20048773.

- Halpern CB, Frenzen PM, Means JE, Franklin JF. 1990. Plant succession in areas of scorched and blown-down forest after the 1980 eruption of Mount St. Helens, Washington. *Journal of Vegetation Science* **1**: 181–194. Available at: www.jstor.org/stable/3235657.
- Hayes SK, Montgomery DR, Newhall CG. 2002. Fluvial sediment transport and deposition following the 1991 eruption of Mount Pinatubo. *Geomorphology* **45**: 211–224. [https://doi.org/10.1016/S0169-555X\(01\)00155-6](https://doi.org/10.1016/S0169-555X(01)00155-6).
- Heimsath AM, Furbish DJ, Dietrich WE. 2005. The illusion of diffusion: field evidence for a depth-dependent sediment transport. *Geology* **33**: 949–952. <https://doi.org/10.1130/G21868.1>.
- Hendrix LB. 1981. Post-eruption succession on Islas Fernandina, Galapagos. *Madrono* **28**: 242–254. Available at: www.jstor.org/stable/41424331.
- Hoblitt RP, Miller CD, Vallance JW. 1981. Origin and stratigraphy of the deposit produced by the May 18 directed blast. In *The 1980 Eruptions of Mount St. Helens*, Washington LPW, Mullineaux DR (eds), US Geological Survey Professional Paper 1250. US Geological Survey: Reston, VA.
- Horton RE. 1945. Erosional development of streams and their drainage basins; hydrophysical approach to quantitative morphology. *Geological Society of America Bulletin* **56**: 275–370. [https://doi.org/10.1130/0016-7606\(1945\)56\[275:EDOSAT\]2.0.CO;2](https://doi.org/10.1130/0016-7606(1945)56[275:EDOSAT]2.0.CO;2).
- Ikeya H, Hendrayanto K, Mizuyama T. 1995. Observed changes in the infiltration rates of pyroclastic deposits resulting from volcanic activities. *Journal of the Japan Society of Erosion Control Engineering* **48**: 22–26 (in Japanese, with English abstract). https://doi.org/10.11475/sabo1973.48.2_22
- Inbar M, Enriquez AR, Graniel JH. 2001. Morphological changes and erosion processes following the 1982 eruption of El Chichon volcano, Chiapas, Mexico. *Geomorphologie: Relief, Processes, Environnement* **3**: 175–183. <https://doi.org/10.3406/morfo.2001.1100>.
- Inbar M, Hubp JL, Ruiz LV. 1994. The geomorphological evolution of the Paricutin cone and lava flows, Mexico, 1943–1990. *Geomorphology* **9**: 57–76. [https://doi.org/10.1016/0169-555X\(94\)90031-0](https://doi.org/10.1016/0169-555X(94)90031-0).
- Janda RJ, Scott KM, Nolan KM, Martinson HA. 1981. Lahar movement, effects, and deposits. In *The 1980 Eruptions of Mount St. Helens, Washington*, Lipman PW, Mullineaux DR (eds), US Geological Survey Professional Paper 1250. US Geological Survey: Reston, VA.
- Kadomura H, Imagawa T, Yamamoto H. 1983. Eruption-induced rapid erosion and mass movements on Usu Volcano, Hokkaido. *Zeitschrift für Geomorphologie Supplement* **46**: 123–142.
- Kadomura H, Yamamoto H, Suzuki R, Suzuki K. 1978. Some aspects of erosional form and processes on tephra-covered hillslopes produced by the 1977 eruption of Usu Volcano, Hokkaido, Japan: August 1977–early August 1978. In *Usu Eruption and its Impact on the Environment*, Hokkaido University, December 1978; 121–139 (in Japanese, with English abstract).
- Kuenzi WD, Horst OH, McGehee RV. 1979. Effect of volcanic activity on fluvial-deltaic sedimentation in a modern arc-trench gap, southwestern Guatemala. *Geological Society of America Bulletin* **90**: 827–838. [https://doi.org/10.1130/0016-7606\(1979\)90<827:EOVAOF>2.0.CO;2](https://doi.org/10.1130/0016-7606(1979)90<827:EOVAOF>2.0.CO;2).
- Lavigne F. 2004. Rate of sediment yield following small-scale volcanic eruptions: a quantitative assessment at the Merapi and Semeru stratovolcanoes, Java, Indonesia. *Earth Surface Processes and Landforms* **29**: 1045–1058. <https://doi.org/10.1002/esp.1092>.
- Lawrence RL, Ripple WJ. 2000. Fifteen years of revegetation of Mount St. Helens: a landscape-scale analysis. *Ecology* **81**: 2742–2752. [https://doi.org/10.1890/0012-9658\(2000\)081\[2742:FYOROM\]2.0.CO;2](https://doi.org/10.1890/0012-9658(2000)081[2742:FYOROM]2.0.CO;2).
- Leavesley GH, Lusby GC, Lichty RW. 1989. Infiltration and erosion characteristics of selected tephra deposits from the 1980 eruption of Mount St. Helens, Washington, USA. *Hydrological Sciences Journal* **34**: 339–353. <https://doi.org/10.1080/02626668909491338>.
- Lehre AK, Collins BD, Dunne T. 1983. Post-eruption sediment budget for the North Fork Toutle River drainage, June 1980–June 1981. *Zeitschrift für Geomorphologie Supplement* **46**: 143–163.
- Lipman PW, Mullineaux DR (eds). 1981. *The 1980 Eruption of Mount St. Helens, Washington*. U.S. Geological Survey Professional Paper 1250. US Geological Survey: Reston, VA.
- Lisle TE. 1995. Effects of coarse woody debris and its removal on a channel affected by the 1980 eruption of Mount St. Helens, Washington. *Water Resources Research* **31**: 1797–1808. <https://doi.org/10.1029/95WR00734>.
- Major JJ. 2004. Posteruption suspended sediment transport at Mount St. Helens: decadal-scale relationships with landscape adjustments and river discharges. *Journal of Geophysical Research* **109**: F01002. <https://doi.org/10.1029/2002JF000010>.
- Major JJ, Mosbrucker AR, Spicer KR. 2018. Sediment erosion and delivery from Toutle River basin after the 1980 eruption of Mount St. Helens: a 30-year perspective. In *Ecological Responses at Mount St. Helens: Revisited 35 Years After the 1980 Eruption*, Crisafulli CM, Dale VH (eds). Springer: New York; 19–44.
- Major JJ, Pierson TC, Dinehart RL, Costa JE. 2000. Sediment yield following severe volcanic disturbance—a two decade perspective from Mount St. Helens. *Geology* **28**: 819–822. [https://doi.org/10.1130/0091-7613\(2000\)28<819:SYFSVD>2.0.CO;2](https://doi.org/10.1130/0091-7613(2000)28<819:SYFSVD>2.0.CO;2).
- Major JJ, Yamakoshi T. 2005. Decadal-scale change of infiltration characteristics of a tephra-mantled hillslope at Mount St Helens, Washington. *Hydrological Processes* **19**: 3621–3630. <https://doi.org/10.1002/hyp.5863>.
- Manville V, Segsneider B, Newton E, White JDL, Houghton BF, Wilson CJN. 2009. Environmental impact of the 1.8 ka Taupo eruption, New Zealand: landscape responses to a large-scale explosive rhyolite eruption. *Sedimentary Geology* **220**: 318–336. <https://doi.org/10.1016/j.sedgeo.2009.04.017>.
- Meyer DF, Martinson HA. 1989. Rates and processes of channel development and recovery following the 1980 eruption of Mount St. Helens, Washington. *Hydrological Sciences Journal* **34**: 115–127. <https://doi.org/10.1080/02626668909491318>.
- Miller JF, Frederick RH, Tracy RJ. 1973. *NOAA Atlas 2, Precipitation-Frequency Atlas of the Western United States, Volume IX—Washington*. US Department of Commerce, NOAA, National Weather Service: Silver Springs, MD.
- Miyabuchi Y, Nakamura F. 1991. Seasonal variation of erosion process at the headwater basin of Obuppu River in Tarumae Volano, Hokkaido. *Transactions, Japanese Geomorphological Union* **12**: 367–377 (in Japanese, with English abstract).
- Miyabuchi Y, Shimizu A, Takeshita K. 1999. Grain size characteristics and infiltration rates of deposits associated with the 1990–95 eruption of Unzen volcano, Japan. *Transactions, Japanese Geomorphological Union* **20**: 85–96 (in Japanese, with English abstract).
- Montgomery DR, Panfil MS, Hayes SK. 1999. Channel-bed mobility response to extreme sediment loading at Mount Pinatubo. *Geology* **27**: 271–274. [https://doi.org/10.1130/0091-7613\(1999\)027<0271:CBMRTE>2.3.CO;2](https://doi.org/10.1130/0091-7613(1999)027<0271:CBMRTE>2.3.CO;2).
- Moody JA, Kinner DA. 2006. Spatial structures of stream and hillslope drainage networks following gully erosion after wildfire. *Earth Surface Processes and Landforms* **31**: 319–337. <https://doi.org/10.1002/esp.1246>.
- Moody JA, Martin DA. 2001. Initial hydrologic and geomorphic response following a wildfire in the Colorado Front Range. *Earth Surface Processes and Landforms* **26**: 1049–1070. <https://doi.org/10.1002/esp.253>.
- Morgan RPC. 1978. Field studies of rainsplash erosion. *Earth Surface Processes* **3**: 295–299. <https://doi.org/10.1002/esp.3290030308>.
- NOAA. 2015. National Centers for Environmental Information. Available at www.ncdc.noaa.gov/
- Ogawa Y, Daimaru H, Shimizu A. 2007. Experimental study of post-eruption overland flow and sediment load from slopes overlain by pyroclastic flow deposits, Unzen volcano, Japan. *Geomorphologie: Relief, Processus, Environnement* **3**: 237–246. <https://doi.org/10.4000/geomorphologie.3962>.
- Ollier CD, Brown MJF. 1971. Erosion of a young volcano in New Guinea. *Zeitschrift für Geomorphologie* **15**: 12–28.
- Ongaro TE, Widiwijayanti AB, Clarke AB, Voight B, Neri A. 2011. Multiphase-flow numerical modeling of the 18 May 1980 lateral blast at Mount St. Helens, USA. *Geology* **39**: 535–538. <https://doi.org/10.1130/G31865.1>.
- Pierson TC. 1985. Initiation and flow behavior of the 1980 Pine Creek and Muddy River lahars, Mount St. Helens, Washington. *Geological Society of America Bulletin* **96**: 1056–1069. [https://doi.org/10.1130/0016-7606\(1985\)96<1056:IAFBOT>2.0.CO;2](https://doi.org/10.1130/0016-7606(1985)96<1056:IAFBOT>2.0.CO;2).

- Pierson TC, Janda RJ, Umbal JV, Daag AS. 1992. *Immediate and long-term hazards from lahars and excess sedimentation in rivers draining Mt. Pinatubo, Philippines*, US Geological Survey Water-Resources Investigations Report 92-4039. US Geological Survey: Reston, VA.
- Pierson TC, Major JJ. 2014. Hydrogeomorphic effects of explosive volcanic eruptions on drainage basins. *Annual Review of Earth and Planetary Sciences* **42**: 469–507. <https://doi.org/10.1007/s00445-013-0723-4>.
- Rathburn SL, Shahverdian SM, Ryan SE. 2018. Post-disturbance sediment recovery: implications for watershed resilience. *Geomorphology* **305**: 61–75. <https://doi.org/10.1016/j.geomorph.2017.08.039>.
- Scott KM. 1988. *Origins, Behavior, and Sedimentology of Lahars and Lahar-runout Flows in the Toutle-Cowlitz River System*, US Geological Survey Professional Paper 1447-A. US Geological Survey: Reston, VA.
- Scott KM, Janda RJ, de la Cruz EG, Gabinete E, Eto I, Isada M, Sexton M, Hadley K. 1996. Channel and sedimentation responses to large volumes of 1991 volcanic deposits on the east flank of Mount Pinatubo. In *Fire and Mud: Eruptions and Lahars of Mount Pinatubo, Philippines*, Newhall CG, Punongbayan RS (eds). Philippine Institute of Volcanology and Seismology/University of Washington Press: Quezon City/Seattle, WA.
- Segerstrom K. 1956. *Erosion Studies at Paricutin, State of Michoacan, Mexico*, US Geological Survey Bulletin 965-A. US Geological Survey: Reston, VA.
- Segerstrom K. 1960. *Erosion and Related Phenomena at Paricutin in 1957*, US Geological Survey Bulletin 1104-A. US Geological Survey: Reston, VA.
- Segerstrom K. 1966. *Paricutin, 1965—Aftermath of Eruption*, US Geological Survey Professional Paper 550-C. US Geological Survey: Reston, VA.
- Shimokawa E, Jitousono T. 1987. Rate of erosion on tephra-covered slopes of volcanoes. *Transactions, Japanese Geomorphological Union* **8**: 269–286 (in Japanese, with English abstract).
- Shimokawa E, Jitousono T, Tsuchiya S. 1996. Sediment yield from the 1984 pyroclastic flow deposit covered hillslopes in Merapi volcano, Indonesia. *Journal of the Japan Society of Erosion Control Engineering* **48**: 101–107. https://doi.org/10.11475/sabo1973.48.Special_101.
- Shimokawa E, Jitousono T, Yazawa A, Kawagoe R. 1989. An effect of tephra cover on erosion processes of hillslopes in and around Sakurajima Volcano. In *Proceedings of the International Symposium on Erosion and Volcanic Debris Flow Technology*, July 31–August 3, Yogyakarta, Indonesia. Ministry of Public Works: Yogyakarta.
- Simon A. 1999. *Channel and Drainage-basin Response of the Toutle River System in the Aftermath of the 1980 Eruption of Mount St. Helens, Washington*, U.S. Geological Survey Open-File Report 96-633. US Geological Survey: Reston, VA.
- Smith RD, Swanson FJ. 1987. Sediment routing in a small drainage basin in the blast zone at Mount St. Helens, Washington, USA. *Geomorphology* **1**: 1–13. [https://doi.org/10.1016/0169-555X\(87\)90003-1](https://doi.org/10.1016/0169-555X(87)90003-1).
- Swanson FJ, Collins B, Dunne T, Wicherski BP. 1983. Erosion of tephra from hillslopes near Mt. St. Helens and other volcanoes. In *Proceedings of the Symposium on Erosion Control in Volcanic Areas, July 6–9, 1982, at Seattle and Vancouver, Washington*. Ministry of Construction, Public Works Institute: Ibaraki.
- Teramoto Y, Shimokawa E. 2010. Temporal changes in vegetation and soil environment caused by volcanic activity of Mount Sakurajima. *Journal of the Japanese Society of Coastal Power* **9**: 59–62.
- Teramoto Y, Shimokawa E, Jitousono T. 2006. Effects of volcanic ash on the runoff process in Sakurajima volcano. In *Disaster Mitigation of Debris Flows, Slope Failures and Landslides*, Marui H (ed). Universal Academy Press: Tokyo.
- Tsuyuzaki S. 1987. Origin of plants on the volcano Usu, northern Japan, since the eruptions of 1977 and 1978. *Vegetatio* **73**: 53–58. <https://doi.org/10.1007/BF00031851>.
- Tsuyuzaki S. 1994. Fate of plants from buried seeds on Volcano Usu, Japan, after the 1977–1978 eruptions. *American Journal of Botany* **81**: 395–399. <https://doi.org/10.1002/j.1537-2197.1994.tb15462.x>.
- Voight B, Glicken H, Janda RJ, Douglass PM. 1981. Catastrophic rockslide avalanche of May 18. In *The 1980 Eruptions of Mount St. Helens, Washington*, Lipman PW, Mullineaux DR (eds), US Geological Survey Professional Paper 1250. US Geological Survey: Reston, VA.
- Waitt RB, Jr. 1981. Devastating pyroclastic density flow and attendant air fall of May 18 – stratigraphy and sedimentology of deposits. In *The 1980 Eruptions of Mount St. Helens, Washington*, Lipman PW, Mullineaux DR (eds), US Geological Survey Professional Paper 1250. US Geological Survey: Reston, VA.
- Waitt RB, Jr. 1989. Swift snowmelt and floods (lahars) caused by great pyroclastic surge at Mount St. Helens volcano, Washington, 18 May 1980. *Bulletin of Volcanology* **52**: 138–157.
- Waitt RB, Jr, Dzurisin D. 1981. Proximal air-fall deposits from the May 18 eruption – stratigraphy and field sedimentology. In *The 1980 Eruptions of Mount St. Helens, Washington*, Lipman PW, Mullineaux DR (eds), US Geological Survey Professional Paper 1250. US Geological Survey: Reston, VA.
- Waldron HH. 1967. *Debris Flow and Erosion Control Problems Caused by the Ash Eruptions of Irazu Volcano, Costa Rica*, US Geological Survey Bulletin 1241-I. US Geological Survey: Reston, VA; 1–37.
- Waythomas CF, Scott WE, Nye JC. 2010. The geomorphology of an Aleutian volcano following a major eruption: the 7–8 August 2008 eruption of Kasatochi Volcano, Alaska, and its aftermath. *Arctic, Antarctic, and Alpine Research* **42**: 260–275. <https://doi.org/10.1657/1938-4246-42.3.260>.
- Wise DR, O'Connor JE. 2016. *A Spatially Explicit Suspended-Sediment Load Model for Western Oregon*, US Geological Survey Scientific Investigations Report 2016-5079. US Geological Survey: Reston, VA.
- Yamakoshi T, Doi Y, Osanai N. 2005. Post-eruption hydrology and sediment discharge at the Miyakejima volcano, Japan. *Zeitschrift für Geomorphologie Supplement* **140**: 55–72.
- Yamakoshi T, Suwa H. 2000. Post-eruption characteristics of surface runoff and sediment discharge on the slopes of pyroclastic-flow deposits, Mount Unzen, Japan. *Transactions, Japanese Geomorphological Union* **21**: 469–497.
- Yamamoto H. 1984. Erosion of the 1977–1978 tephra layers on a slope of Usu volcano, Hokkaido. *Transactions, Japanese Geomorphological Union* **5**: 111–124 (in Japanese, with English abstract).
- Zheng S, Wu B, Thorne CR, Simon A. 2014. Morphological evolution of the North Fork Toutle River following the eruption of Mount St. Helens, Washington. *Geomorphology* **208**: 102–116. <https://doi.org/10.1016/j.geomorph.2013.11.018>.
- Zobel DB, Antos JA. 1992. Survival of plants buried for eight growing seasons by volcanic tephra. *Ecology* **73**: 698–701. <https://doi.org/10.2307/1940777>.